Promoted V2O5/TiO2 catalysts for selective catalytic reduction of NO with NH3 at low temperatures

Putluru, Siva Sankar Reddy; Schill, Leonhard; Godiksen, Anita; Poreddy, Raju; Mossin, Susanne; Jensen, Anker Degn; Fehrmann, Rasmus

Published in:
Applied Catalysis B: Environmental

Link to article, DOI:
10.1016/j.apcatb.2015.10.044

Publication date:
2016

Document Version
Peer reviewed version

Title: Promoted V_2O_5/TiO_2 catalysts for selective catalytic reduction of NO with NH_3 at low temperatures

Author: Siva Sankar Reddy Putluru Leonhard Schill Anita Godiksen Raju Poreddy Susanne Mossin Anker Degn Jensen Rasmus Fehrmann

PII: S0926-3373(15)30225-3
DOI: http://dx.doi.org/doi:10.1016/j.apcatb.2015.10.044
Reference: APCATB 14351

To appear in: *Applied Catalysis B: Environmental*

Received date: 16-7-2015
Revised date: 9-10-2015
Accepted date: 21-10-2015

Please cite this article as: Siva Sankar Reddy Putluru, Leonhard Schill, Anita Godiksen, Raju Poreddy, Susanne Mossin, Anker Degn Jensen, Rasmus Fehrmann, Promoted V2O5/TiO2 catalysts for selective catalytic reduction of NO with NH3 at low temperatures, Applied Catalysis B, Environmental http://dx.doi.org/10.1016/j.apcatb.2015.10.044

Promoted V_2O_5/TiO_2 catalysts for selective catalytic reduction of NO with NH_3 at low temperatures

Siva Sankar Reddy Putluru[1], Leonhard Schill[1], Anita Godiksen[1], Raju Poreddy[1], Susanne Mossin[1], Anker Degn Jensen[2] andRasmus Fehrmann[*1].

[1]*Centre for Catalysisand Sustainable Chemistry, Department of Chemistry, Building 207, Technical University of Denmark, DK-2800 Kgs. Lyngby, Denmark*

[2]*Combustion and Harmful Emission Control Research Centre, Department of Chemical and Biochemical Engineering, Building 229, Technical University of Denmark, DK-2800 Kgs. Lyngby, Denmark*

Graphical abstract

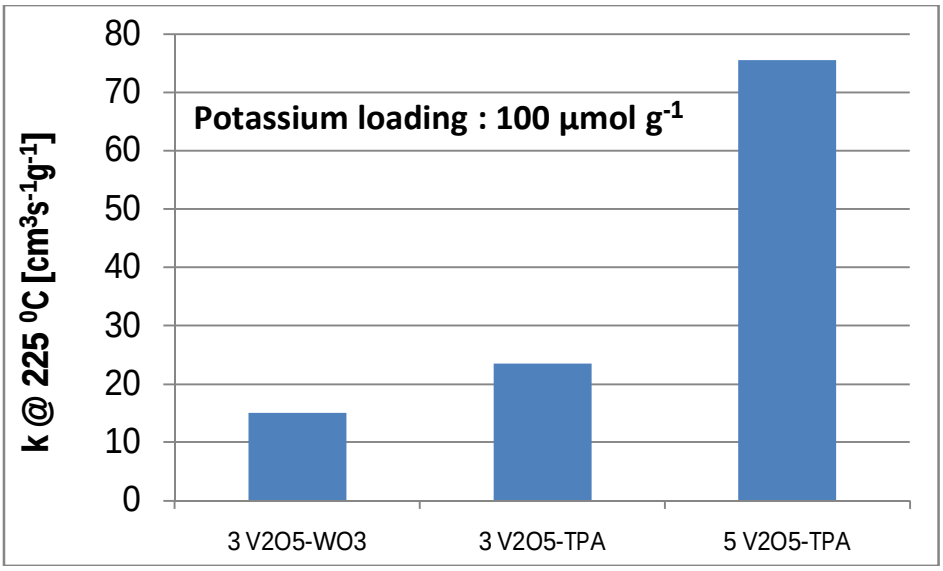

Highlights

- Increased low temperature deNOx activity by increasing vanadia loading (3 to 6 wt.%)
- Increased K tolerance by increasing vanadia loading from 3 to 6 wt.%.
- Increased K tolerance by using heteropoly acids instead of WO_3.

Abstract

The influence of varying the V_2O_5 content (3-6 wt.%) was studied for the selective catalytic reduction (SCR) of nitrogen oxides by ammonia on heteropoly acid (HPA)- and tungsten oxide (WO_3)-promoted V_2O_5/TiO_2 catalysts. The SCR activity and alkali deactivation resistance of HPA-promoted V_2O_5/TiO_2 catalysts was found to be much higher than for WO_3- promoted catalysts. By increasing the vanadium content from 3 to 5 wt.% the catalysts displayed a two fold increase in activity at 225 °C and retained their initial activity after alkali doping at a molar K/V ratio of 0.181. Furthermore, the catalysts were characterized by N_2 physisorption, XRPD, NH_3-TPD, H_2-TPR, Raman, FTIR and EPR spectroscopy to investigate the properties of the catalysts. XRPD, Raman and FTIR showed that promotion with 15 wt.% HPA does not cause V_2O_5 to be present in crystalline form, also at a loading of 5 wt.% V_2O_5. Hence, use of HPAs does not cause increased N_2O formation or unselective oxidation of NH_3. NH_3-TPD showed that promotion by HPA instead of WO_3 causes the catalysts to possess a higher number of acid sites, both in fresh and alkali poisoned form, which might explain their higher potassium tolerance. *Ex-situ* EPR spectroscopy revealed that HPA-promoted catalysts have a higher V^{4+}/V_{total} ratios than their WO_3-promoted counterparts. H_2-TPR suggests that HPAs do not have a beneficial effect on the V^{5+}-V^{3+} redox system, relative to WO_3.

Keywords: SCR of NO with NH_3; V_2O_5; Potassium poisoning

* Corresponding author. Tel.: +45 45252389; fax: +45 45883136.

E-mail address: rf@kemi.dtu.dk (R. Fehrmann)

1. Introduction

The selective catalytic reduction (SCR) of NO with NH_3 is widely employed for reduction of NO_x emissions from stationary sources like gas, oil and coal-fired power plants. The most well-known and commercially applied catalyst is vanadium well-dispersed on a titania support and promoted by WO_3- (V_2O_5-WO_3/TiO_2) [1-3]**.** The commercial catalyst has high activity and N_2 selectivity in NH_3-SCR at 300-400 °C. To achieve this temperature the commercial catalysts are usually placed in the high-dust position, since the low dust-position in the flue gas stream requires reheating of the flue gas [4].

Applying NH_3-SCR for flue gas cleaning from biomass and waste incineration plants demands a highly active catalyst, which is able to withstand the high content of ash (impurities include K, Na and Ca) and SO_2 in the flue gas. The rate of deactivation is especially high for biomass and waste incineration plants [5, 6], and therefore the tail-end configuration downstream of the flue gas desulphurization unit is recommended.

At the tail-end position the lower levels of SO_2 in the flue gas allow the use of catalyst formulations with higher V_2O_5 contents and the low levels of dust allow the use of monoliths with a high geometric surface area. Further, the lifetime of the catalyst

is increased due to less deposition of dust and ammonium sulfates [7]. However, for tail-end configuration it is necessary to install a more active catalyst capable of providing sufficient conversion at lower temperatures (approximately 200-250 °C). Thereby a minimum reheating of the flue gas should be applied. It is known that the selectivity towards N_2 during SCR conditions is a function of operating temperature and content of vanadium [1]. Thus at low operating temperatures catalysts with more reactive formulations (higher content of vanadium, promoters etc.) might be operated without compromising the selectivity towards N_2.

Over the last decade there has been a great interest in the development of low-temperature SCR catalysts containing transition metal oxides such as Mn-Fe/TiO_2 [7, 8] and V_2O_5/TiO_2 [9-11]. Active formulations containing metals other than vanadium have not been widely commercialized because of issues with selectivity and sensitivity to SO_2. Also there has been much attention towards developing a highly active vanadium formulation using sol-gel [9], deposition precipitation [10] and sequential impregnation methods via high surface area titania hydrate carriers [11]. The sol-gel method affords catalysts with up to 20 wt.% vanadia which have shown excellent potassium tolerance. However, the synthesis is relatively elaborate which might make its industrial implementation difficult. Recently, it has been reported that increasing the vanadia loading of catalysts prepared by impregnation can result in increased potassium tolerance [12-13]. Another approach is to use HPAs promoters instead of the commonly used WO_3. The majority of catalytic applications use the most stable and easily available Keggin type HPAs e.g. $H_3PW_{12}O_{40}$, $H_4SiW_{12}O_{40}$ and $H_3PMo_{12}O_{40}$. In our previous publications we reported the promotional effect of HPAs, for NH_3-SCR of NO_x [14-15]. Combining

the use of HPAs [14-15] with increased vanadia loadings [12-13] could be a promising and relatively easily implementable approach. However, there are some open questions such as: (i) Will an increase in the vanadia content change the HPAs structure and reduce its acidity? (ii) Will the presence of HPAs allow high vanadia loadings to be present in non-crystalline form? (iii) Will HPAs adversely affect the V^{5+}-V^{3+} redox system? (iv) Will N_2O be formed at increased rates? All these issues can have a large effect on the activity and potassium tolerance and therefore merit further experimental investigation.

In the present work, 3-6 wt.% V_2O_5 was studied for NH_3-SCR of nitrogen oxides on Keggin type HPAs and WO_3-promoted V_2O_5/TiO_2 catalysts. The deactivation effect of potassium additives on the SCR activity was studied on 3 and 5 wt.% V_2O_5 catalysts, since even at tail-end position there may be a small amount of aerosols that could poison the catalyst. Optimum catalysts were characterized by various techniques to obtain a detailed understanding of the SCR performance.

2. Experimental

2.1 Catalyst preparation and characterization

HPA- and WO_3-promoted V_2O_5/TiO_2 catalysts were prepared as described previously [14]. Briefly, anatase-supported HPAs $H_3PW_{12}O_{40}$ (TPA), $H_4SiW_{12}O_{40}$ (TSiA), and $H_3PMo_{12}O_{40}$ (MPA) (Aldrich, 99.9%) were prepared by suspending a known amount of dried TiO_2 anatase powder (Aldrich, 99.9%) in aqueous solutions of the corresponding HPA The suspension mixture (optimum HPA loading, 15 wt.%) was dried at 120 °C for 12 h [14-15]. Similarly, 10 wt.% WO_3-TiO_2 was prepared by incipient wetness impregnation using ammonium metatungstate (Fluka, 99%) as a precursor on

anatase TiO_2. The 10 wt.% WO_3-TiO_2 was dried and calcined at 500 °C for 5 hours. This temperature was chosen because former studies on HPA-promoted catalysts have shown that calcination at higher temperatures reduces the catalytic activity [14].

3-6 wt.% V_2O_5 modified catalysts were prepared by wet impregnation of the HPA-TiO_2 and 10 wt.% WO_3-TiO_2 supports with 0.5-1.2 M vanadium oxalate solutions. The vanadium oxalate solutions were prepared from ammonium meta-vanadate and oxalic acid (Aldrich, 99.9%) in the molar ratio 1:2 at 70 °C. The obtained HPA-V_2O_5/TiO_2 catalysts were dried and calcined for 4 hours at 400 °C and the WO_3-promoted V_2O_5/TiO_2 catalysts were calcined at 450 °C for 4 hours.

The potassium-doped catalysts were prepared by subsequent wet impregnation with a solution of KNO_3 (Sigma-Aldrich, 99.9%) to obtain a potassium loading of 100 µmol/g catalyst, corresponding to molar K/V ratios of 0.303 and 0.181 for 3 and 5 wt.% V_2O_5, respectively. The potassium-doped catalysts were oven-dried at 100 ^oC for about 2 hours and then calcined for 4 hours at 400 °C.

XRPD measurements were performed on a Huber G670 powder diffractometer using CuK_α radiation within a 2θ range of 2-80° in steps of 0.02°. BET surface areas of the samples (100 mg catalyst) were determined from nitrogen physisorption measurements at liquid nitrogen temperature with a Micromeritics ASAP 2010 instrument.

FTIR spectra of the samples were recorded on a Perkin Elmer 1710 spectrometer at ambient conditions in KBr disks (1 mg in 100 mg). Raman spectra were measured by microscopic confocal Raman Spectrometer (Renishaw plc, UK) under

ambient conditions using a LEXEL 95-SHG-QS Argon-ion laser (from Cambridge Laser Laboratories Inc., California, USA) as a light source with a wavelength of 488 nm. The spectra were recorded with a resolution of 1 cm^{-1} and a scan number of 20 from 200-1200 cm^{-1}.

EPR: The catalyst samples were transferred directly into a dessicator after calcination and stored there until the measurement. *Ex-situ* EPR spectra were recorded on approximately 20 mg sample at room temperature in a 4mm suprasil quartz EPR tube using a continuous wave X-band Bruker EMX-EPR spectrometer with the ER 4102ST cavity and a gun diode microwave source. The microwave power was 6.5 mW, modulation frequency 100 kHz, modulation amplitude 8 G, microwave frequency 9.4-9.7 GHz. 2048 points were summed up over 4 scans in the interval 240-450 mT. Data treatment was performed with Matlab using EasySpin 4.5.3 [16]. Reference spectra for spin quantification were recorded with identical instrument settings on known solid solutions of $VOSO_4$ in K_2SO_4.

NH_3-TPD experiments were conducted on a Micromeritics Autochem-II instrument. In a typical TPD experiment, 100 mg of sample was placed in a quartz tube and pretreated in helium flow at 100 ℃ for 1 hour. The sample was treated with anhydrous NH_3 gas (Air Liquide, 5% NH_3 in He) at 100 °C. After NH_3 adsorption, the sample was flushed with helium (50 mL/min) for 1 hour at 100 °C. Finally, the TPD operation was carried out by heating the sample from 100 to 600 °C (10 °C /min) under a flow of helium (50 mL/min).

H_2-TPR studies were conducted on a Micromeritics Autochem-II instrument. In a typical experiment, 100 mg of sample was placed in one arm of a U-shaped quartz sample tube on a quartz wool plug. The TPR analysis was carried out in a reducing mixture (50 mL/min) consisting of 4% H_2 and balance Ar (Air Liquide) from 50 °C to 850 °C (10 °C/min). The hydrogen concentration in the effluent stream was monitored by a thermal conductivity detector (TCD) and the H_2 consumption was calculated from calibration experiments.

2.2 Catalytic activity measurements

The SCR activity measurements were carried out at atmospheric pressure in a fixed-bed reactor loaded with 50 mg of fractioned (180-300 µm) catalyst at a flow rate of 300 NmL/min(at room temperature). This corresponds to a space velocity of about 180,000 h^{-1} assuming a density of 0.5 g mL^{-1} of a monolith in an industrial application. This is about 20 to 40 times higher than the typical real life space velocities. We chose a higher space velocity in the screening experiments for the following reasons: (i) Industrial catalyst (in monolithic form) suffers from mass transport limitations; (ii) High NO_x reductions (i.e. 90%) are required and (iii) Deactivation over a lifetime of 5-10 years needs to be allowed for. The inlet concentrations were: NO = 1000 ppm, NH_3 = 1000 ppm, O_2 = 4% and H_2O = 2.3% with He as balance gas. During the experiments the temperature was increased stepwise from 125 to 300 °C while the NO and NH_3 concentrations were continuously monitored by a Thermo Electron Model 17C chemiluminescent NH_3-NO_x gas analyzer. At each set-temperature the N_2O concentration was further measured by gas chromatography (Shimadzu-14 B GC, TCD detection,

poraplot column). The NO conversion (%) was measured after attaining steady state, approximately 45 min at each temperature.

3. Results and discussion

The results of N_2-BET surface area are shown in Table 1. The surface area of the $3V_2O_5$10WO_3-TiO_2, $3V_2O_5$TPA-TiO_2, $3V_2O_5$TSiA-TiO_2, and $3V_2O_5$MPA-TiO_2 catalysts was found to be 103, 112, 114 and 96 m^2/g, respectively. The surface area of the $5V_2O_5WO_3$-TiO_2, $5V_2O_5$TPA-TiO_2, $5V_2O_5$TSiA-TiO_2 and $5V_2O_5$MPA-TiO_2 catalysts was found to be 99, 105, 106 and 90 m^2/g, respectively. With an increase in metal loading from 3 to 5 wt.% V_2O_5, a slight decrease in surface area is noticed.

The X-ray powder diffraction (XRPD) patterns of 3 and 5 wt.% V_2O_5 catalysts are shown in Fig. 1. No peaks attributable to crystalline V_2O_5, WO_3, or HPA phases were observed, only support TiO_2 phases were observed indicating that the vanadium and promoters are highly dispersed on the support. The detection limit of the XRPD apparatus is around 5 nm, and any crystalline particles would be undetected below this size. Dominant anatase (2θ = 25.3°, 37.9°, 47.8° and 54.3°) and a very small amount of the rutile (2θ = 27.4°˚, 36.1° and 54.2°) phases are present in the catalysts. The decrease in surface area with increasing V_2O_5 loading from 3 to 5 wt.% suggests that crystalline TiO_2 is covered with an amorphous V_2O_5 surface leading to some pore blocking.

It is well known that the SCR reaction requires NH_3 to adsorb on the catalyst. The adsorption capacity and desorption patterns as a function of temperature are greatly influenced by the surface acidity of the SCR catalysts. Promotors such as WO_3 or MoO_3 on the TiO_2 support increase the acidity and mechanical strength. In the present

investigation, the acidity of the catalysts was measured using the NH_3-TPD method. Even though this method is not able to discriminate between Brønsted- and Lewis-acid, it still gives valuable information regarding the total number and strength of the acid sites. The NH_3-TPD profiles of V_2O_5TPA-TiO_2, V_2O_5TSiA-TiO_2, V_2O_5MPA-TiO_2 and $V_2O_5WO_3$-TiO_2 catalysts are shown in Fig. 2 a) and Fig. 2 b). Figure 2 c) shows the total number of acid sites as a function of promoter. All the fresh catalysts show broad NH_3-desorption patterns from 150 to 650 °C. The total amount of adsorbed ammonia, which is determined from the area under the TPD curve, corresponds to weakly adsorbed ammonia (desorption temperature below 200 °C) and strongly adsorbed ammonia (desorption temperature above 300 °C). These sites originate from the TiO_2 support, promoters (WO_3 or heteropoly ions) and vanadium present in the catalyst. It is observed that the desorption peaks for the HPA-promoted catalysts (100- 550 °C) are broader compared to the WO_3-promoted catalysts (100- 400 °C). Pure and TiO_2-supported HPAs were previously reported to be super acidic [14]. The super acidic nature of HPAs is due to their discrete and mobile ionic structure, which is tunable through the chemical composition. The NH_3-TPD results are summarized in Table 1.

The fresh, HPA-promoted samples possess significantly more acid sites than the WO_3-promoted ones, regardless of the vanadia loading. Increasing the vanadia loading from 3 to 5 wt.% causes the total number of acid sites of $V_2O_5WO_3$-TiO_2 and V_2O_5TPA-TiO_2 to increase by 40 and 144 μmol g^{-1}, respectively. The total number of acid sites of V_2O_5TSiA-TiO_2 and V_2O_5MPA-TiO_2 decrease by 20 and 121 μmol g^{-1}, respectively.

Figure 2 also shows the NH_3-TPD profiles of potassium-doped catalysts (100 µmol /g of potassium) as dotted lines. A significant decrease in total peak area and intensity of strongly adsorbed ammonia peaks are observed. All the potassium-doped catalysts showed above stoichiometric (moles of adsorbed NH_3/moles of K) loss of surface acid sites. The $3V_2O_5$TPA-TiO_2, $3V_2O_5$TSiA-TiO_2 and $3V_2O_5$MPA-TiO_2 catalysts lost 339 -412 µmol/g of acid sites, whereas the $3V_2O_5WO_3$-TiO_2 catalyst lost only 126 µmol/g of acid sites. $5V_2O_5$TPA-TiO_2 and $5V_2O_5$TSiA-TiO_2 lost 432 and 404 µmol/g of acid sites, respectively, which is close to the losses of the corresponding 3 wt.% vanadia samples. $5V_2O_5$TPA-TiO_2 lost only 141 µmol/g. This makes it a promising candidate. The result was confirmed by reproducing the potassium impregnation step. The $5V_2O_5WO_3$-TiO_2 catalyst lost 161 µmol/g of acid sites which is close to the value of $3V_2O_5WO_3$-TiO_2. Above stoichiometric loss of acid sites can be explained by a recently reported deactivation mechanism. Here, one potassium metal atom can deactivate up to four vanadium atoms [17] and if we also consider impact of potassium on vanadia and titania the atomic ratio of K:V:Ti is 1:2:4 [18]. It is expected that promoters are decreasing the impact of potassium on the active V-OH sites, which are responsible for initiating the SCR reaction through ammonia adsorption. The HPAs probably provide sacrificial acid sites as was reported earlier [14].

In order to study the redox properties of catalysts, H_2-TPR measurements were performed. The TPR profiles of 3 wt.% V_2O_5 and 5 wt.% V_2O_5 catalysts are shown in Fig. 3 a) and Fig. 3 b), respectively. The catalysts show three reduction peaks between

450-480 °C (assigned to the reduction of $V^{5+}$to V^{3+}), 600-630 °C (assigned to the W^{6+} reduction to $W^{4+}$from WO_3, TPA and TSiA or Mo^{6+} reduction to Mo^{4+} from MPA) and 740-790 °C (assigned to the further reduction of W^{4+} or Mo^{4+} to W^0or Mo^0), respectively [11, 19]. The difference in reduction temperatures for the catalysts is due to the combined effect of the vanadium content, promotor formulations and constituent elements associated in HPAs. By increasing the V_2O_5 content from 3 to 5 wt.% an increase in the intensity of the vanadium reduction peak can be observed around 450 °C. Figure 3 c) shows the (V^{5+} to V^{3+}) peak temperatures of both fresh and poisoned catalysts and Figure 3 d) gives the peak shifts due to K. Fresh catalysts loaded with 5 wt.% V_2O_5 reduce at slightly higher temperatures than the corresponding 3 wt.% samples. This is probably due to the formation of slightly bigger vanadia particles at higher loadings. Potassium doping causes pronounced peak shifts. In the case of WO_3-, TPA- and TSiA-promoted catalysts the shifts are little affected by the vanadia loading. The MPA-promoted catalyst, however, shows a significantly lower shift at the higher vanadia loading. This, together with the high retention of acid sites, is expected to result in lower reduction of the SCR activity. The poisoned, WO_3-promoted samples show V^{5+} to V^{3+} reduction temperatures close to the ones of the HPA-promoted counterparts. The peaks assigned to the reduction of W^{4+} or Mo^{4+} to W^0or Mo^0 shift very little due to K doping.

FTIR spectra of the V_2O_5TPA-TiO_2, V_2O_5TSiA-TiO_2, V_2O_5MPA-TiO_2 and $V_2O_5WO_3$-TiO_2 catalysts along with support patterns are shown in Fig. 4. Pure V_2O_5

spectra show stretching mode of V=O (vanadyl) at 1020 cm^{-1} and the V-O-V stretching mode at 830 cm^{-1} [10]. Except for the pure V_2O_5 all catalysts display a broad band in the region between 3200-3600 cm^{-1} and a sharp peak at 1620 cm^{-1}, which are due to the stretching and bending vibrations of O-H groups, respectively. The peak at 1400 cm^{-1} and the bands below 800 $cm^{-1}$are due to the Ti-O-Ti stretching vibrations.

Metal-oxygen stretching modes of the Keggin units are mainly present in the 650-1150 cm^{-1} range. In the literature the most common assignments reported for pure TPA, TSiA and MPA are given as: TPA shows bands at 1081 (P-O), 982 (W=O), 888 and 804 cm^{-1} (W-O-W) [20], TSiA shows bands at 1021 (Si-O-Si), 984 (W=O), 928 (Si-O), 885, and 791 cm^{-1} (W-O-W) [21] and MPA shows bands at 1065 (P-O), 963 (Mo=O), 869 and 793 cm^{-1} (Mo-O-Mo) [22]. The V_2O_5TPA-TiO_2, V_2O_5TSiA-TiO_2 and V_2O_5MPA-TiO_2 catalysts display similar bands in the 1082-962 cm^{-1} region indicating that the Keggin structure is maintained after impregnation. The lower wave number bands (lower than 900 cm^{-1}) are covered with intense broad vibration peaks originating from Ti-O-Ti bonds [20]. The $V_2O_5WO_3$-TiO_2 catalyst shows a band at 977 cm^{-1} which is associated with the W=O stretching of the tungstyl species [23]. The vanadyl species are not detected because of their low concentrations compared to the promoters and the support.

Raman spectroscopy was applied in order to understand the molecular structure of the HPAs, tungstyl and vanadyl species. HPAs typically show symmetric (ν_s) and asymmetric (ν_{as}) vibrations of: terminal oxygen ($\nu(M=O_t)$), corner shared bridged oxygen ($\nu(M-O_b-M)$), edge shared bridged oxygen ($\nu(M-O_c-M)$) and oxygen in the central tetrahedron ($\nu(Mo-O_a)$) with M being W, Mo, P or Si. Characteristic Raman peaks of the bulk $H_3PW_{12}O_{40}$ (TPA) were reported at 1007, 991, 982 and 902 cm^{-1}, which were

attributed to $\nu_s(W=O_t)$, $\nu_{as}(W=O_t)$, $\nu(P-O_a)$ and $\nu(W-O_b-W)$, respectively [24-25]. Similarly, bulk $H_4SiW_{12}O_{40}$(TSiA) exhibited bands at 1002, 980, 922 and 881 cm^{-1} due to $\nu_s(W=O_t)$, $\nu_{as}(W=O_t)$, $\nu(Si-O_a)$ and $\nu(W-O_b-W)$, respectively [25-26]. Raman spectra of pure $H_3PMo_{12}O_{40}$ (MPA) was reported with bands at 996, 983, 882, 606 and 246 cm^{-1} which were assigned to $\nu_s(Mo=O_t)$, $\nu_{as}(Mo=O_t)$, $\nu_s(Mo-O_b-Mo)$, $\nu_s(Mo-O_c-Mo)$ and $\nu_s(Mo-O_a)$ [27]. Raman spectra of bulk WO_3 are expected to show bands at 808, 714 and 276 cm^{-1} and were assigned to the W=O stretching mode, the W=O bending mode, and the W-O-W deformation mode respectively [28]. Raman spectra of bulk V_2O_5 bands are reported at 993, 703, 405 and 285 cm^{-1} [29]. Crystalline V_2O_5 was reported to give a sharp band at 994 cm^{-1} [30]. This is very close to some of the bands of $H_3PW_{12}O_{40}$ (TPA) (980 cm^{-1}), $H_4SiW_{12}O_{40}$(TSiA) and $H_3PMo_{12}O_{40}$ (MPA) (996 and 983 cm^{-1}).

The molecular structure of the supported species depends on the loading and the sample pre-treatment during measurement. The Raman bands at 1007, 992 and 1008 cm^{-1} correspond to the TPA, MPA and TSiA, respectively, see Fig. 5. Since the bands are not sharp it is unlikely that they represent crystalline V_2O_5. The presence of the same Raman bands in the spectra for the V_2O_5-HPA-TiO_2 catalysts and for the bulk HPAs indicate that the Keggin structure of the HPA remain stable upon impregnation on TiO_2. The stable structure of the HPAs is further supported by the absence of bands of the individual oxides, i.e., WO_3 or MoO_3, which would appear upon decomposition of the Keggin structure at 808 and 818 cm^{-1}, respectively [28, 31]. This observation as well as the NH_3-TPD results given above indicates that increasing the vanadium content from 3 to 5 wt.% does not compromise the structure of poly acids.

The signal at 1026 cm^{-1} observed for all the catalysts can be assigned to isolated surface vanadium oxide species [11, 30]. The position of the Raman bands are the same after increasing the V_2O_5 content from 3 to 5 wt.%. Furthermore, increasing the vanadia loading does not increase the intensity of the band at around 990-1010 cm^{-1} relative to the band at around 1026 cm^{-1}, which would be the case if significant amounts of crystalline V_2O_5 were formed. In corroboration with the XRD results this shows that the nature of the vanadia species has not changed significantly. Therefore, unselective oxidation of ammonia and increased N_2O formation are not expected under the SCR conditions used in this study.

Recently [32] a direct correlation between high surface V^{4+}/V^{5+} ratio (derived from *ex-situ* XPS measurements) and SCR activity has been reported. In order to investigate the prevalence of reduced vanadium in the catalysts we proceeded to use EPR spectroscopy to probe the V^{4+} state. EPR spectroscopy is a powerful technique for detecting the paramagnetic V^{4+} species in vanadium catalysts. Fig. S2 and S3 show the EPR spectra of fresh and poisoned 3 and 5 wt.% V_2O_5 catalysts recorded at room temperature. The total amount of V^{4+} was determined by comparison of the double integral of the EPR signal of the sample to the signal of a series of V^{4+} standard samples. The results are shown in Fig. 6. The V^{4+} content of fresh samples varies a lot and is lowest in the WO_3 containing catalyst, irrespective of the vanadia loading, and higher in especially the MPA- and TPA-doped catalysts. The higher content of V^{4+} in HPAs-doped catalysts could be another reason for their higher activities. Potassium causes the difference between the $3V_2O_5$-TiO_2 promoted with WO_3 and HPAs to become almost

negligible. The poisoned $5V_2O_5$-TiO_2 catalysts reveal larger differences. The WO_3-promoted one contains only 2.2% V^{4+} compared to the total vanadium content while the MPA-promoted one contains 8.0%. Whether these differences also exist under *in-situ* conditions (elevated temperatures, presence of ammonia and NO) might be investigated in the future.

The spin Hamiltonian parameters were determined by simulations in EasySpin and are listed in Table 2 (detailed information and figures in S1, S2 and S3). From this it is seen that approximately 88% of the EPR signal on all catalysts is found in a broad isotropic line with g = 1.97 and a peak-to-peak width of 250 G. This species is similar to that observed for pure crystalline V_2O_5, and is assigned to tetragonal 5- or 6-coordinated vanadyl VO^{2+} species [33] The line broadening is due to the amorphous nature of the sites as well as spin-spin interactions with neighboring V^{4+} sites.

Species **A** with well-defined sharp lines in the EPR spectrum has spin Hamiltonian parameters of $g_\perp$ = 1.97, $g_\parallel$= 1.90, $A_\perp$ = 208 MHz and $A_\parallel$ = 560 MHz. This species can be assigned to a well-defined and magnetically isolated 6-coordinate vanadyl species [34, 35]. Another species, **B** also with sharp lines has parameters that are very similar to species **A**. Although the local coordination around vanadium is different enough to give a distinct set of peaks it is still assigned as a tetragonal vanadyl species.

Figure 7 shows the NO conversion (%) profiles of 3-6 wt.% V_2O_5TPA-TiO_2, V_2O_5TSiA-TiO_2, V_2O_5MPA-TiO_2 and $V_2O_5WO_3$-TiO_2 catalysts as a function of the

reaction temperature. At temperatures below 175 °C, the catalysts exhibit low NO conversion, higher conversion is observed above 200 °C and almost full conversion is seen at 300 °C. Fig. 7(a, b and c) shows that a gradual increase in V_2O_5 loading enhances the NO conversion which reaches a maximum at 5 wt.% V_2O_5 and a further increase of the V_2O_5 loading leads to a gradual decrease of NO conversion. Figure 7(d) also shows that a gradual increase in V_2O_5 loading enhances the NO conversion and almost similar conversion profiles were observed for 5 and 6 wt.% V_2O_5. For a fair comparison with other catalysts we considered the 5 wt.% V_2O_5 as the optimum $V_2O_5WO_3$-TiO_2 catalyst.

It is interesting to see the NO conversion (%) of the catalysts loaded with 3 and 5 wt.% V_2O_5. The difference in NO conversion between these samples is apparent at the intermediate temperature 225 °C, where the catalysts are just active enough to initiate the reaction. $3V_2O_5$TPA-TiO_2, $3V_2O_5$TSiA-TiO_2, $3V_2O_5$MPA-TiO_2 and $3V_2O_5WO_3$-TiO_2 exhibited NO conversions of 28.9, 28.8, 30.6 and 27.1%, respectively. By comparison with the samples with 5 wt.%: $5V_2O_5$TPA-TiO_2, $5V_2O_5$TSiA-TiO_2, $5V_2O_5$MPA-TiO_2 and $5V_2O_5WO_3$-TiO_2 exhibited a NO conversion of 53.8, 51.6, 43.9 and 42.1%, respectively. Overall, an almost two fold increase in activity is observed by increasing the V_2O_5 content from 3 to 5 wt.%. Similar observations were reported for WO_3-promoted high surface area titania hydrate on 1.5, 3 and 5 wt.% V_2O_5 catalysts [11].

SCR catalysts are expected to be sufficiently selective so that minimal or no N_2O formation occurs. It is known that at sufficiently high temperatures, N_2O formation occurs from the partial oxidation of ammonia in the presence of an SCR catalysts. Especially at relatively high reaction temperatures (i.e.> 400 °C) this is an issue even for low content V_2O_5 catalysts (1-3 wt.%) [36]. Under the current experimental conditions

(i.e with 2.3 vol.% water), it should be mentioned that even for the 6 wt.% V_2O_5 catalysts no traces of N_2O were detected throughout the investigated temperatures.

Doping the catalysts with potassium (100 µmol/g) resulted in a decrease in the SCR activity (Fig. 8). At 225 °C, K-3V_2O_5TPA-TiO_2, K-3V_2O_5TSiA-TiO_2, K-3V_2O_5MPA-TiO_2 and K-3$V_2O_5$$WO_3$-$TiO_2$ catalysts displayed NO conversion of 23.4, 23.3, 28.4 and 15.1%, respectively. Increasing the V_2O_5 loading to 5 wt.% the K-5V_2O_5TPA-TiO_2, K-5V_2O_5TSiA-TiO_2, K-5V_2O_5MPA-TiO_2 and K-5$V_2O_5$$WO_3$-$TiO_2$ catalysts displayed NO conversions of 54.6, 48.9, 45.2 and 38.8%, respectively.

The K-3V_2O_5TPA-TiO_2, K-3V_2O_5TSiA-TiO_2, K-3V_2O_5MPA-TiO_2 and K-3$V_2O_5$$WO_3$-$TiO_2$ catalysts retained 81, 80, 92 and 55% of the initial activity, respectively. The 5 wt.% V_2O_5 loaded K-5V_2O_5TPA-TiO_2, K-5V_2O_5TSiA-TiO_2, K-5V_2O_5MPA-TiO_2 and K-5$V_2O_5$$WO_3$-$TiO_2$ catalysts performed with 100, 95, 100 and 92% of their initial activity, respectively. Replacing WO_3 with HPAs is obviously a fruitful approach also at a relatively high vanadia loading of 5 wt.%.

4. Conclusions

Promoting V_2O_5/TiO_2 with 15 wt.% HPA instead of 10 wt.% WO_3 increases the potassium tolerance at 225 °C at both 3 and 5 wt.% vanadia. This is most probably due to a higher number of surface acid sites left after potassium poisoning as shown with NH_3-TPD. Redox properties, on the other hand, seem not to be generally enhanced by HPAs as shown by H_2-TPR. The combination of high vanadia loadings (5 wt.%) with HPAs does not induce the formation of crystalline V_2O_5 as confirmed by XRD, FTIR and Raman spectroscopy. Therefore, unselective oxidation of ammonia and N_2O formation are not higher than in the WO_3-promoted case. *Ex-situ* EPR studies have shown that the V^{4+}/V_{total}

ratio is higher in HPA-promoted catalysts than in the WO_3-promoted counterparts. The differences are more pronounced for the fresh catalysts and might give an additional explanation for the promotional effect of HPAs. Future studies could comprise optimization of both HPAs and vanadia loadings as well as the effect of higher potassium loadings. Furthermore, investigation of the thermal stability of HPAs- and WO_3-promoted catalysts at temperatures above 300 °C could be of interest in order to assess the viability of the former under high-dust conditions.

Acknowledgements

This work is financially supported by Energinet.dk through the PSO project 10521. Rolf W. Berg is gratefully acknowledged for assisting with the Raman measurements.

References

[1] L.J. Alemany, L. Lietti, N. Ferlazzo, P. Forzatti, G. Busca, E. Giamello, F. Bregani, J. Catal.,155 (1995) 117
[2] V.I. Parvulescu, P. Grange, B. Delmon, Catal. Today, 46 (1998) 233.

[3] P. Forzatti, Appl.Catal. A., 222(2001) 221
[4] H. Bosch, F. Janssen, Catal. Today., 2 (1988) 489.
[5] K. Wieck-Hansen, P. Overgaard, O.H. Larsen, Biomass Bioenergy., 19 (2000) 395.
[6] R. Khodayari, C.U.I. Odenbrand, Ind. Eng.Chem. Res., 37 (1998) 1196.
[7] L. Schill, S.S.R. Putluru, R. Fehrmann, A.D. Jensen, CatalLett., 144 (2014) 395.
[8] R. Jin, Y. Liu, Y. Wang, W. Cen, Z. Wu, H. Wang, Z. Wenig, Appl. Catal. B., 148-149 (2014) 582.
[9] S.B. Kristensen, A.J. Kunov-Kruse, A. Riisager, S.B. Rasmussen, R. Fehrmann, J. Catal.,284 (2011) 60
[10] S.S.R. Putluru, L. Schill, D. Gardini, S. Mossin, J.B. Wagner, A.D. Jensen, R. Fehrmann, J. Mater. Sci., 49 (2014) 2705.
[11] P.G.W.A. Kompio, A. Brückner, F. Hipler, G. Auer, E. Löffler, W. Grünert, J. Catal., 286 (2012) 237.
[12] C. Chen, X. Wu, W. Yu, Y. Gao, D. Weng, L. Shi, C. Geng, Chin. J. Catal., 36 (2015) 1287-1294
[13]S. Xiaoyan, Ding Shipeng, H. Hong, L. Hanqiang, L. Guangjie,
Chin. J. Env. Engineering (2014) 8, 2031-2034
[14] S.S.R. Putluru, A.D. Jensen, A. Riisager, R. Fehrmann, Catal. Sci. Technol., 1 (2011) 631.
[15] S.S.R. Putluru, S. Mossin, A. Riisager, R. Fehrmann, Catal. Today 176 (2011) 292.
[16] S. Stoll, A. Schweiger, ´EasySpin, a comprehensive software package for spectral simulation and analysis in EPR' J. Magn. Reson. 178 (2006) 42-55
[17] D. Nicosia, I. Czekaj, O. Kröcher, Appl. Catal. B., 77 (2008) 228.
[18] A.E. Lewandowska, M. Calatayud, E. Lozano-Diz, C. Minot, M.A. Bañares, Catal. Today.,139 (2008) 209.
[19] L. Lizama, T. Klimova, Appl. Catal. B., 82 (2008) 139.
[20] G. Marcì, E. Garcìa-López, M. Bellardita, F. Parisi, C. Colbeau-Justin, S. Sorgues, L.F. Liotta,
L. Palmisano, Phys. Chem. Chem.Phys., 15 (2013) 13329.
[21] M.N. Blanco, L.R. Pizzio, Appl. Surf. Sci., 256 (2010) 3546.
[22] T.R. Zhang, W. Feng, Y.Q. Fu, R. Lu, C.Y. Bao, X.T. Zhang, B. Zhao, C.Q. Sun, T.J. Li, Y.Y. Zhao, J.N. Yao, J. Mater. Chem., 12 (2002) 1453
[23] G. Cristallo, E. Roncari, A. Rinaldo, F. Trifirò, Appl. Catal. A., 209 (2001) 249.
[24] L. Nakka, E. Molinari, I.E. Wachs, J. Am. Chem. Soc., 131 (2009) 15544
[25] R.M. Ladera, M. Ojeda, J.L. Fierro, S. Rojas, Catal.Sci. Technol., 5 (2015) 484.
[26] J.A. Rengifo-Herrera, R.A. Frenzel, M.N. Blanco, L.R. Pizzio, J. Photoch. Photobiol. A., 289 (2014) 22
[27] H. Atia, U. Armbruster, A. Martin, J. Catal., 258 (2008) 71
[28] E.I. Ross-Medgaarden, I.E. Wachs, J. Phys. Chem. C., 111(2007) 15089
[29] C. Sanchez, J. Livage, G. Lucazeau, J. Raman. Spectrosc., 12 (1982) 68
[30] M.A. Vuurman, I.E. Wachs, A.M. Hirt, J. Phys. Chem., 95 (1991) 9928
[31] M. Li, J. Shen, X. Ge, X. Chen, Appl. Catal. A., 206 (2001) 161
[32] T. Boningari, R. Koirala, P. G. Smirniotis, Appl. Catal. B., 140-141 (2013) 289-298
[33] O.B. Lapina, A.A. Shubin, A.V. Nosov, E. Bosch, J. Spengler, H. Knözinger,

J. Phys. Chem. B., 103 (1999)7599
[34] G. Centi, S. Perathoner, F. Trifiro, A. Aboukais, C.F. Aissi, M. Guelton,
J. Phys Chem. Vol. 96 (1992) 2617
[35] L. Lietti, J.L. Alemany, P. Forzatti, G. Busca, G. Ramis, E. Giamello, F. Bergani,
Catal.Today 29 (1996) 143.
[36] S. Djerad, L. Tifouti, M. Crocoll, W. Weisweiler, J. Mol. Catal. A., 208 (2004) 257.

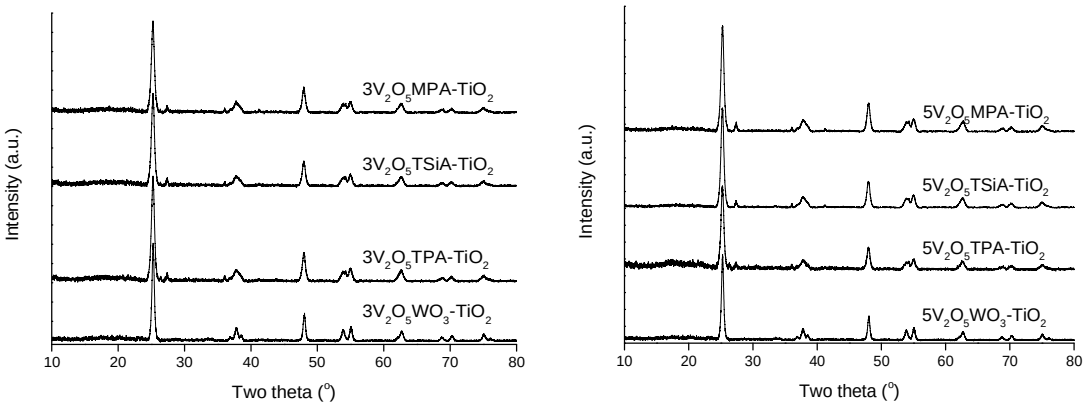

Fig. 1 XRPD patterns of 3 and 5 wt.% V_2O_5 catalysts.

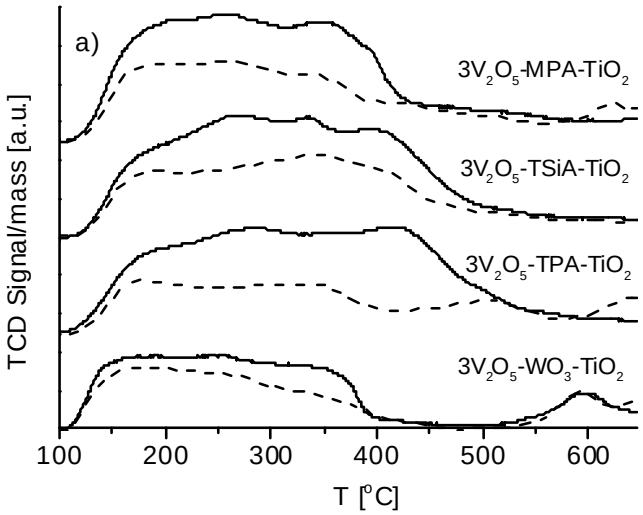

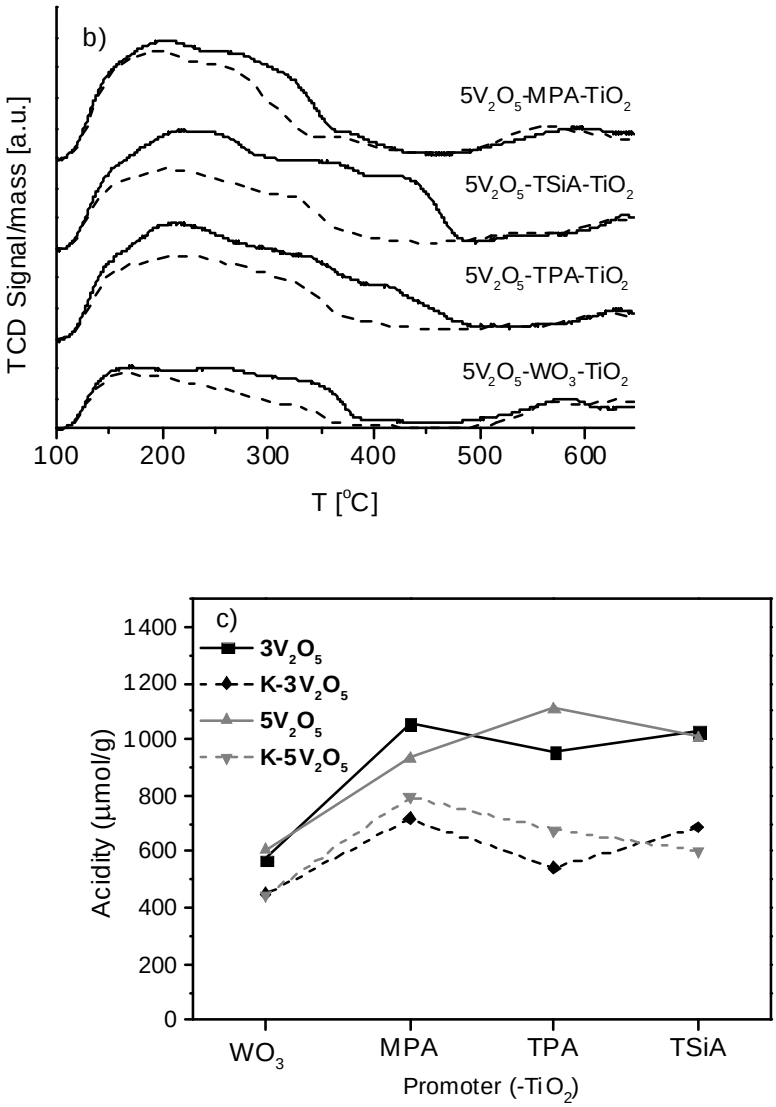

Fig. 2 NH_3-TPD profiles of fresh (straight lines) and potassium-doped (dotted lines); a) 3 wt.% V_2O_5 catalysts, b) 5 wt.% V_2O_5 catalysts, c) total number of acid sites.

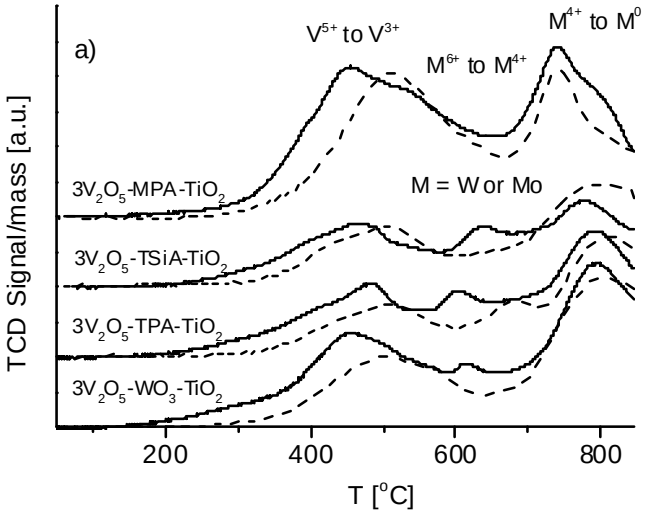

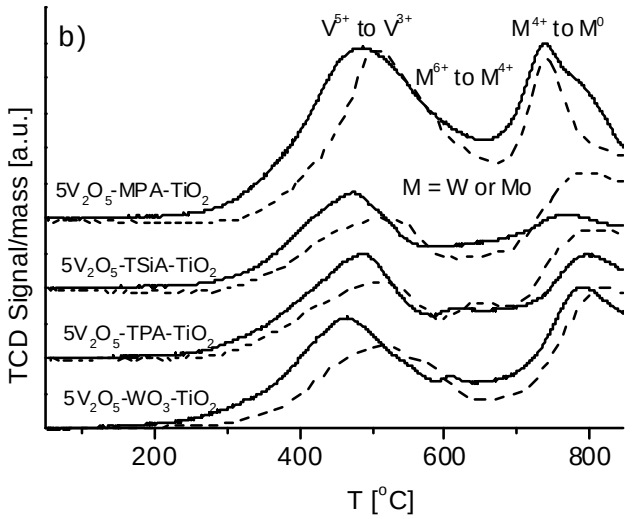

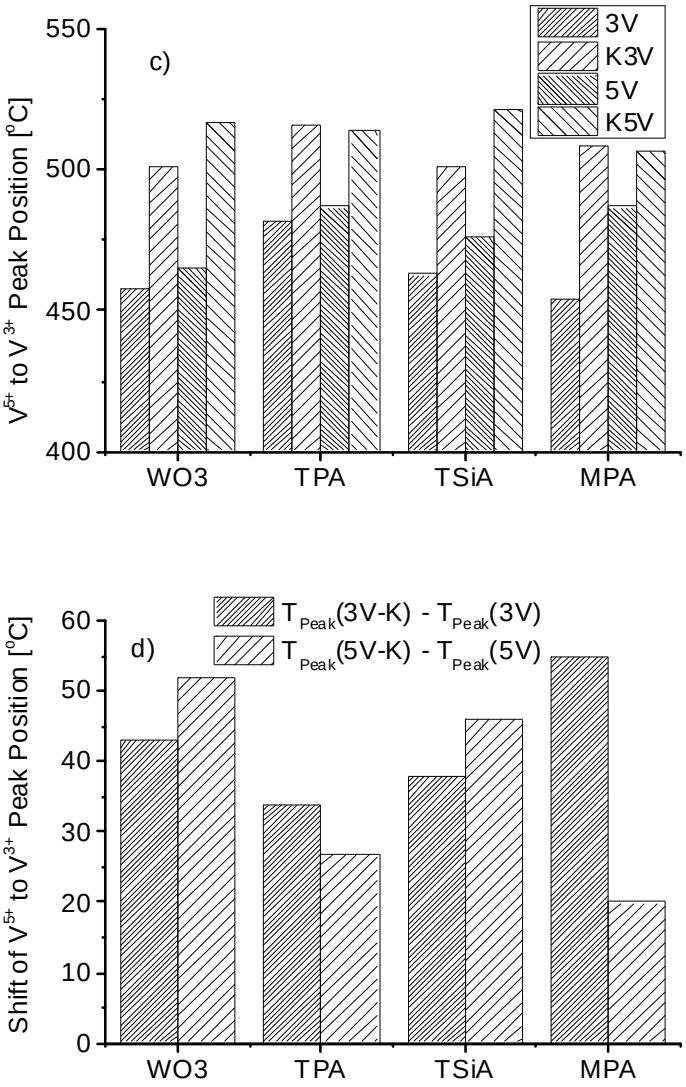

Fig. 3 H_2-TPR profiles of fresh (straight lines) and potassium-doped (dotted lines); a) 3 wt.% V_2O_5 catalysts, b) 5 wt.% V_2O_5 catalysts, c) peak positions of V^{5+} to V^{3+} reduction, d) shift of peak positions of V^{5+} to V^{3+} reduction upon K poisoning.

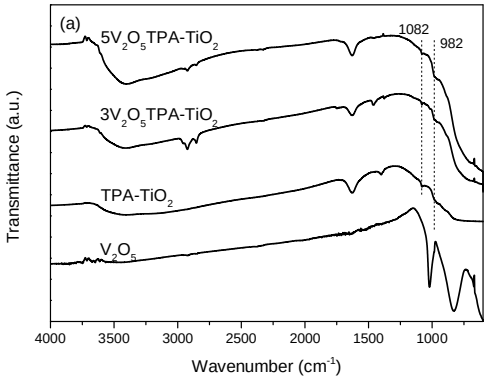

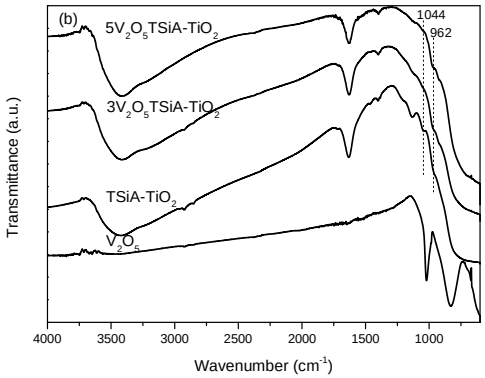

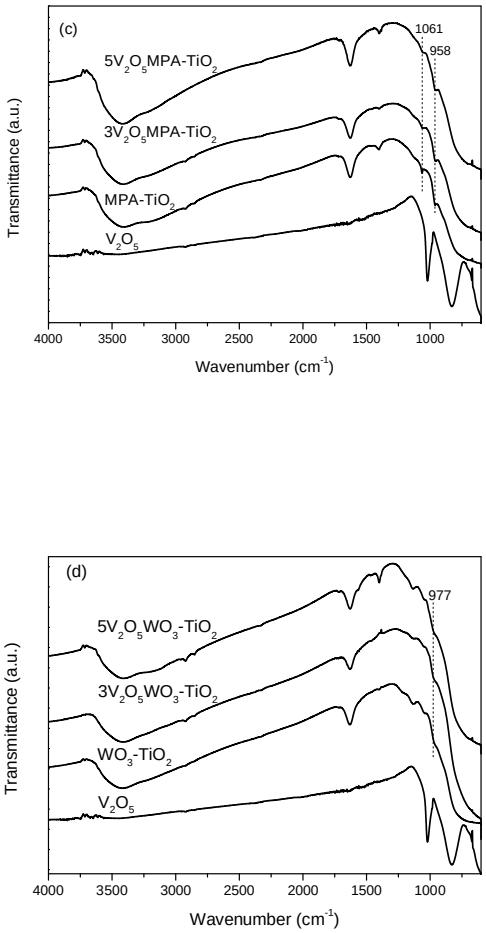

Fig. 4 FTIR spectra of TPA-, TSiA-, MPA- and WO_3-promoted V_2O_5/TiO_2 catalysts.

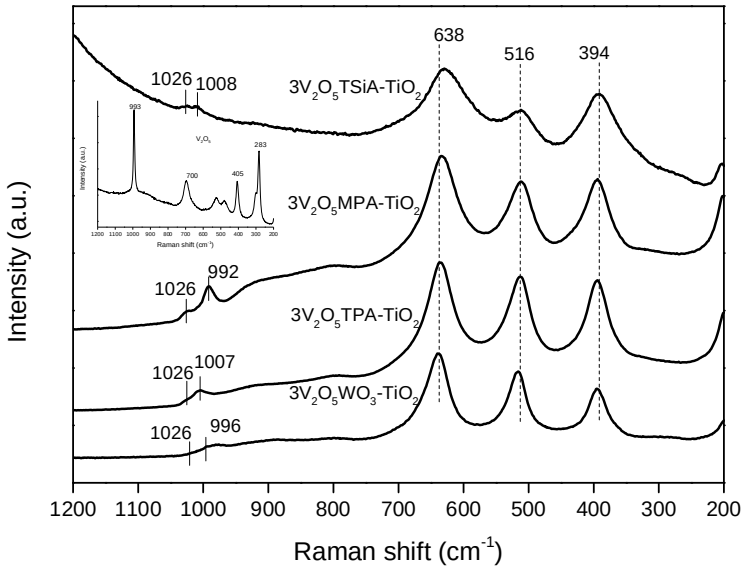

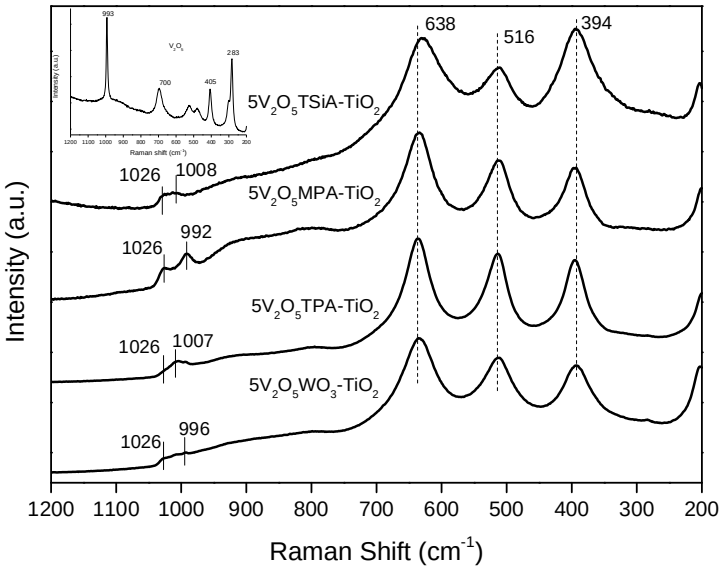

Fig. 5 Raman spectra of 3 and 5 wt.% V_2O_5 catalysts.

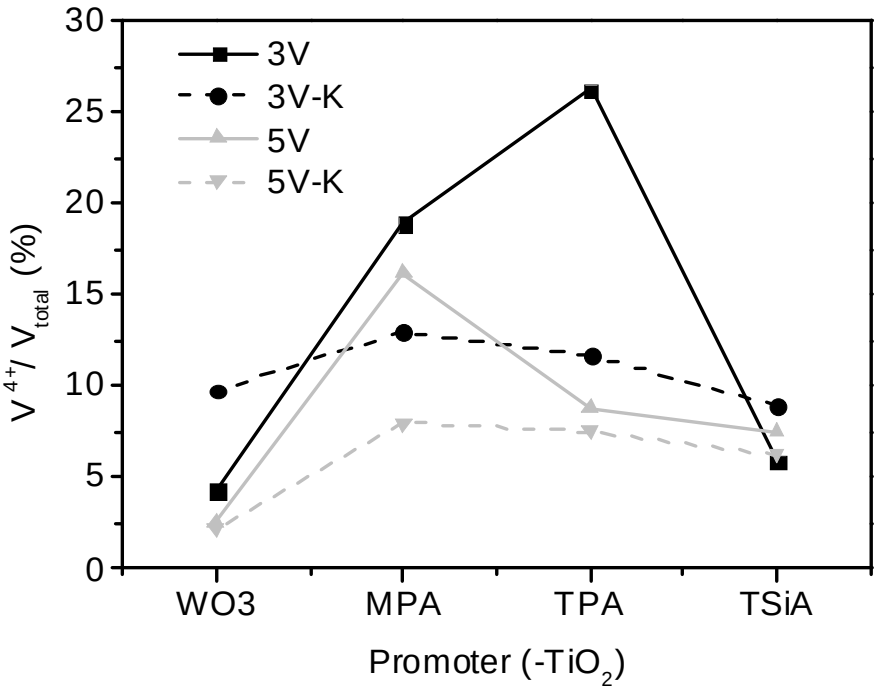

Fig. 6 V^{4+} content as determined by EPR.

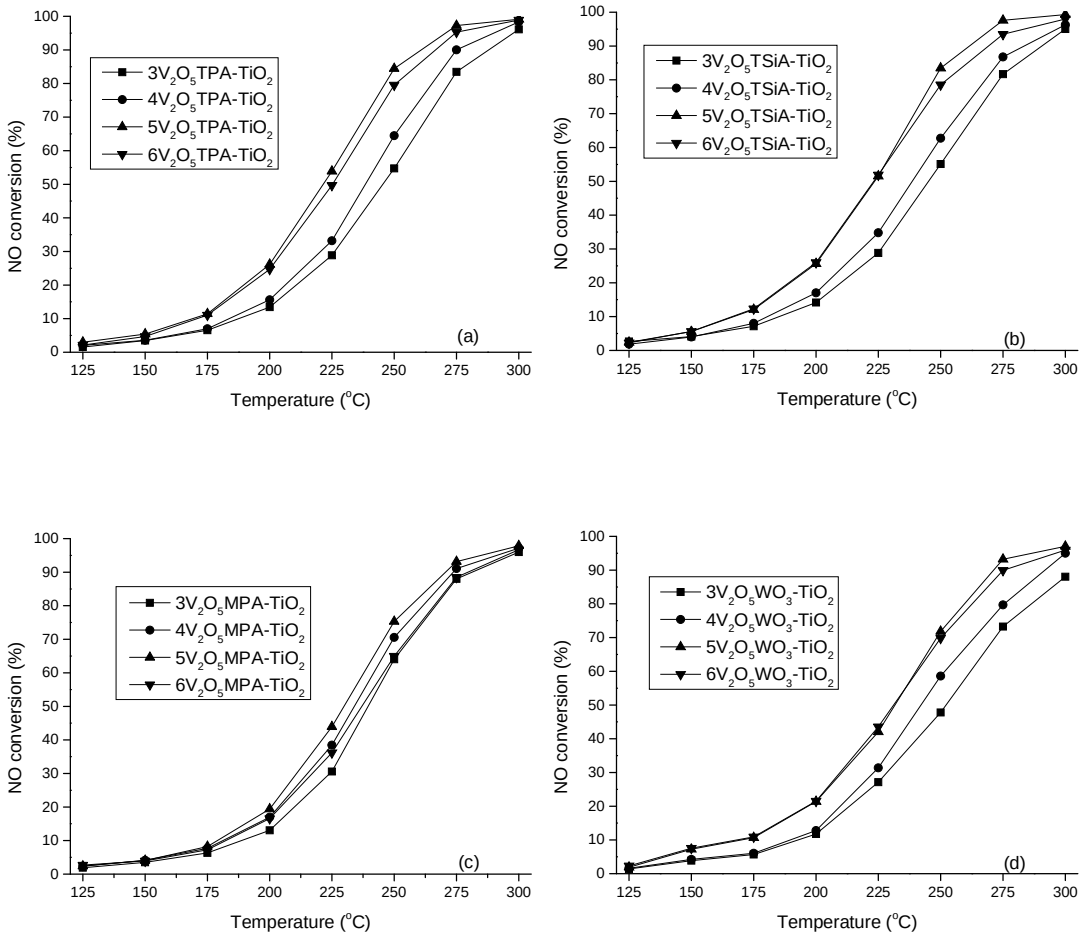

Fig. 7 SCR activity of 3-6 wt.% V_2O_5 catalysts.

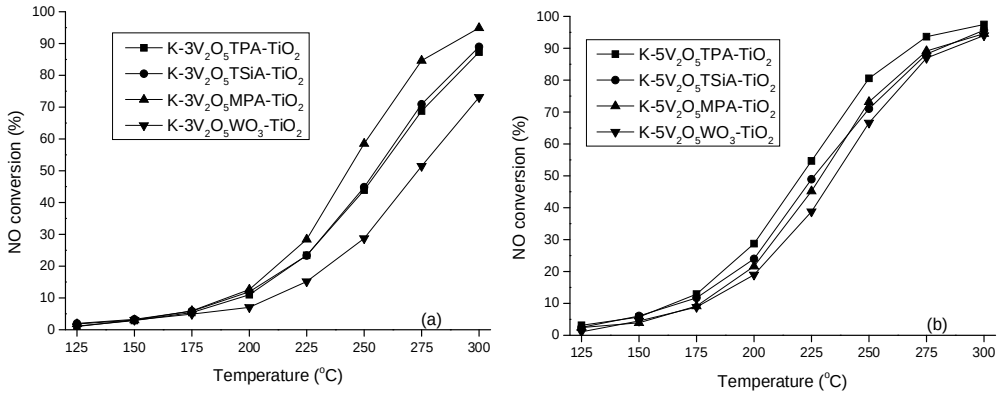

Fig. 8 SCR activity of potassium-doped 3 and 5 wt.% V_2O_5 catalysts.

Table 1 Physico-chemical properties of the catalysts.

Catalyst	Surface area	Acidity [μmol/g]		Acidity loss [μmol/g]	Stochiometry of acidity loss [mol NH_3/mol K]
	Fresh	Fresh	K-doped		
$3V_2O_5WO_3$-TiO_2	103	574	448	126	1.26
$3V_2O_5$TPA-TiO_2	112	955	543	412	4.12
$3V_2O_5$TSiA-TiO_2	114	1028	687	341	3.41
$3V_2O_5$MPA-TiO_2	96	1056	717	339	3.39
$5V_2O_5WO_3$-TiO_2	99	608	447	161	1.61
$5V_2O_5$TPA-TiO_2	105	1111	679	432	4.32
$5V_2O_5$TSiA-TiO_2	106	1008	604	404	4.04
$5V_2O_5$MPA-TiO_2	90	935	794	141	1.41

Table 2 Simulated spin hamiltonian parameters and their distribution. Individual parameters are found in S1 and simulation plots in S2.

Sample		**V^{4+} Site Distribution (%)**		
		A	**B**	**C**
		$g_{\perp}$ = 1.97±0.01 $A_{\perp}$ = 206±5 $g_{\|\|}$ = 1.90±0.01 $A_{\|\|}$ = 570±20	$g_{\perp}$ = 1.97±0.01 $A_{\perp}$ = 182±9 $g_{\|\|}$ = 1.92±0.01 $A_{\|\|}$ = 534±26	g = 1.97±0.01 unresolved A
$3V_2O_5WO_3$-TiO_2		9.2	6.0	84.8
$5V_2O_5WO_3$-TiO_2		9.5	13.8	76.8
$3V_2O_5$TPA-TiO_2		7.1	4.1	88.8
$5V_2O_5$TPA-TiO_2		6.5	4.8	88.7
$3V_2O_5$TSiA-TiO_2		8.0	7.0	85.0
$5V_2O_5$TSiA-TiO_2		5.9	4.4	89.7
$3V_2O_5$MPA-TiO_2		6.7	4.4	88.9
$5V_2O_5$MPA-TiO_2		7.9	2.9	89.2